



Alexandria University
Alexandria Engineering Journal

www.elsevier.com/locate/aej
www.sciencedirect.com



Union is Strength: Improving face sketch synthesis by fusing outcomes of Fully-Convolutional-Networks and Random Sampling Locality Constraint



Irfan Azhar^a, Mudassar Raza^a, Muhammad Sharif^{a,*}, Seifedine Kadry^b,
Seungmin Rho^{c,*}

^a Department of Computer Science, COMSATS University Islamabad, Wah Campus 47040, Pakistan

^b Department of Applied Data Science, Noroff University College, Kristiansand, 4612, Norway

^c Department of Industrial Security, Chung-Ang University, Seoul 06974, Korea

Received 24 August 2021; revised 11 February 2022; accepted 4 April 2022

KEYWORDS

Face recognition;
Fast-RSLCR technique;
FCN technique;
Image fusion;
NLDA;
Photo Sketch synthesis

Abstract Automated formulation of sketches from face photos has seen successive growth since the work of Wang and Tang in recent years. Each new methodology is, however, able to partially achieve its objective of sketch synthesis while using pairs of photos and viewed sketches as a training medium. The viewed sketches are also used as a testing medium to determine the success of those methodologies. Resulting sketches do not fully capture all features of the training photos and viewed sketches. Their similarity value to respective sketch is also around 30 – 50%. One technique may produce sketches with sharp edges, but they do not bear completeness of facial features. Another technique produces sketches with the completeness of facial elements, but they are not well-focused. Second limitation of existing techniques is attributable to face-recognition procedure which is used as a validation step for these methodologies. Face-recognition process with help of synthesized sketches delivers reliable results over datasets with a limited diversity of age, ethnicity, and light intensities. We propose a novel and cost-effective approach to fuse resulting sketches of two test techniques. The two techniques are merged to yield a better sketch containing well-defined features, sharp contours, and less noise. Secondly, fusion suppresses limitations of the component methodologies reaching the resulting sketch. To test this idea of combining sketch-synthesis methods, we experiment with the most basic techniques of image fusion including simple (arithmetic), PCA, and Wavelet based fusions. The proposed setup considered FCN (complete features but less sharpness) and Fast-RSLCR (sharp edges but missing contours) as candidate techniques. It is tested on two datasets namely CUFS and CUFSF. Second dataset incorporates variations of age, ethnicity, light intensities, and slightly deformed features between photos and viewed

* Corresponding authors.

E-mail addresses: irfanazhar_cui@ciitwah.edu.pk (I. Azhar), mudassaraza@ciitwah.edu.pk (M. Raza), sharif@ciitwah.edu.pk (M. Sharif), seifedine.kadry@noroff.no (S. Kadry), smrho@cau.ac.kr (S. Rho).

Peer review under responsibility of Faculty of Engineering, Alexandria University.

<https://doi.org/10.1016/j.aej.2022.04.007>

1110-0168 © 2022 THE AUTHORS. Published by Elsevier BV on behalf of Faculty of Engineering, Alexandria University
This is an open access article under the CC BY-NC-ND license (<http://creativecommons.org/licenses/by-nc-nd/4.0/>).

sketches. Our results indicate achievement of 60.29% SSIM score (enhancement by 3.84%) and 79.03% face-recognition score (enhancement by 5.62%) as compared to Fast-RSLCR.

© 2022 THE AUTHORS. Published by Elsevier BV on behalf of Faculty of Engineering, Alexandria University This is an open access article under the CC BY-NC-ND license (<http://creativecommons.org/licenses/by-nc-nd/4.0/>).

1. Introduction

Automated synthesis of face sketches [1–5] applies to domains of online entertainment [6] face recognition [7–11] and legal purposes [12]. Face images acquired from the security and surveillance tapes are used by police and other agencies. Usually, these images are of low resolution, poor quality, occluded, and/or blurred [13]. As an alternative, sketches are drawn by forensic artists upon clues provided by eye-witnesses or the artist's examination of the subject or security tapes [14]. Other purposes include but not limited to: (a) identification of persons who are victims of accidents, and their faces are not fit for classical photography and (b) search of missing persons where relevant or most recent photographs are not available. These sketches then help in the identification and search of the suspect or wanted individuals. We consider it useful to formulate an arrangement where a photo database is converted to sketch domain by an algorithm trained on viewed sketches by a particular artist. Therefore, a forensic sketch by the same artist would be tested against that database of synthesized sketches carrying his style. This intra-domain comparison would also constitute a validation step of our work involving face-recognition procedure.

Image-based techniques of generating sketches fail to translate the drawing style of a sketch artist. Therefore, it results in sketches being more resembling the original photos [15]. Synthesis by example-based techniques can capture subtle properties of the photos which are identifying characteristics. These features are also given importance by sketch artists who highlight them by shadows, strokes, accentuation, and other drawing parameters. Exemplar-based methods work with datasets containing pairs of the photos and their corresponding viewed-sketches. Tang and Wang [16,17] set the foundation for the synthesis of sketches based on face photos. They used principal component analysis to match test photos with candidate patches from the training dataset. Target sketches are formulated by the linear addition of those patches. Coefficients are computed from the linear relationship between test photos and the training photos. In this process minute and defining features of the test-photo are lost because they are not translated to the resulting sketch which is blurred. To address the deficiencies of pioneer work, novel techniques were put forth. A comparative analysis of all such methodologies is given in [18] which may be referred to for detail study. Here we mention related work post-March 2017.

The conventional hand-engineered based approaches have been the focus for computer vision based methods including sketch synthesis. Zhang and Ji [19] employed a previous concept of active appearance model to synthesize sketches from photos using Eigen transformation as the conversion medium. Their work is however restricted to basic facial features only and it did not include glasses, earrings, or other external ele-

ments of the face. Radman A. and Suandi [20] introduced a completely novel method of synthesizing a pseudo-sketch from the photo. Their work employed simple arithmetic functions and morphological operations on a single photo to generate its pseudo-sketch. This technique does not involve any training or testing scheme. Reliable extraction of hair masks is relatively a weak area of this methodology. Jiang et al [21] also tested a novel idea of using residual image which is difference of the photo and its viewed sketch in the exemplar domain of face-sketch synthesis. The neural network and its variants including deep learning building blocks [22] e.g. convolutional neural networks (CNN) [23–29], Long Short Term Memory (LSTM) [30] and Autoencoders [31,32] have proved themselves a good choice for many domains of computer vision. Some neural network based approaches in the context of face sketches are discussed in the following text. The work of Zhang et al [33] focused on translating identity specific and common information from face image to the sketch by employing two complex structures collectively termed as Markov Random Neural Fields (MRNF). It gave comparative results with other methods by using two face-recognition techniques and it showed higher performance due to visually improved textures of the sketches. Jiao et al [34] explored the use of neural-network composed of two convolutional, pooling, and multilayer perceptron layers to synthesize a sketch from a photo. It was observed that computationally this synthesis scheme is relatively light-weight since it did not involve complex optimization problems like conventional example-based methods. It produced sketches with competitive scores of quality parameters as compared to exemplar-based methods. This work, however, did not conduct face recognition procedure as a validation step to establish the existence of a superior edge and contour information of its resulting images. Zhang et al [35] proposed a modified adversarial generative network called pGAN which consisted of four different stages. Its novelty lay in use of a parametric sigmoid function in the overall process and addition of illumination layer to the intermediate sketch. Moreover, the authors experimented with training the network with one dataset and testing it by another. Therefore, it could generate sketches from photos in the wild like those of celebrities. Our proposed methodology considers the next two contributions to the field of photo-sketch synthesis. Zhang et al [36] proposed a model of sketch synthesis called Fully Convolutional Network (FCN) based on a convolution neural network. In that method whole photo is used as input and the network captures relationships between a person's identity characteristics from the photo and their translation to sketch by the viewed artist. This method benefits from generative discriminative minimization in the post-processing stage. This methodology, however, fails to maintain the sharpness of shapes and edges. Lu et al [37] proposed model of face sketch synthesis by employing a combination of FCN and

exemplar based approaches. Chen et al [38] proposed a model of face sketch synthesis based on a group of three elements of Deep Learning. They demonstrated their arrangement could learn intricate details of sketches and then it could produce sketches from photos outside the training dataset. Wang et al [39] introduced a model called Random Sampling and Locality Constraint (RSLCR) and its improved version (Fast-RSLCR) based on offline random sampling against online K-NN search to synthesize a sketch. This method works well on one dataset, but its results are not equally superior on second dataset which contained more diversity than the first dataset. In the abovementioned discussion we have seen that different methodologies follow procedures that are customized and well-suited to specific purposes. On the other hand, each one of them, however, involves a minor or major problem. Therefore, any given method of photo-sketch formulation does not meet all requirements as stipulated by the gold standard of a viewed sketch.

We propose to unite strong points of existing algorithms in a way that resulting sketch bears distinct features, sharp edges, well-defined contours, and least noise. The main contribution is discussed as follows:

- i. To demonstrate our proposed scheme, we chose two techniques FCN [36] and Fast-RSLCR [39] to mitigate their weaknesses by considering and combining their strong points.
- ii. We unite the sketch-based result of these techniques by six different algorithms such as simple union-based fusion, PCA based fusion, and four variations of wavelet-based fusion.
- iii. The outcome fusion images are applied to face sketch similarity and recognition using SSIM and NLDA respectively for performance evaluation of the proposed approach.

The rest of this paper is organized as follows. We first delineate problems of existing methodologies in Section 2. Our proposed scheme of operation is given in Section 3. Experimentation, results, and their analysis are discussed in Section 4. Concluding remarks and options for future work are mentioned in Section 5.

2. Problems of existing techniques

Image generation by convolution network suffers from Border Effect which produces dark patches on the edges of resulting images. Therefore, to address that issue, FCN [36] paper introduced cropping of the images. Convolution operations reduce the feature map. An increasing number of layers further shrink feature domain. One solution to this problem is the addition of padded information on the edges of an image under process before convolution operations but such an arrangement introduces border effect [40]. Therefore, padding was not added to images during the training and testing phases. As a result, actual images of 155 * 200 shrank to (143 * 188) in the process. The second limitation of the convolutional technique used by FCN to generate sketches is its inability to render sharp edges and clear contours of features. This inadequacy is also observed when we compare its result with synthesized sketches

of [17]. Lack of sharp edges in the result of FCN indicates the absence of high-frequency components in the generated sketches. This omission deprives the sketch of its distinctive features. Moreover, it also means the sketch is vulnerable to its chief characteristics being missed during verification and recognition processes. FCN technique was used on only one publicly available database called The Chinese University of Hong Kong (CUHK) Face sketch database termed as CUFS in its separate and original contributor [17]. CUHK is composed of photos of Asiatic ethnicity with the minimum variation of age and facial features. Authors of FCN also mentioned that their given technique might be employed in a dataset covering the diversity of age, race, facial features, and occlusions like glasses, earrings, etc. A comparative analysis of existing techniques of photo sketch generation is given in [18]. Comparison is based on sketches generated by different techniques when employed to two datasets including CUFS comprising 606 images and CUFSF consisting of 1025 images, both publicly provided by [17]. The latter dataset contains requisite diversity of age, race, and facial features. Moreover, these sketches are more exaggerated in appearance, and they contain intentional deformations and differences in details with respect to their corresponding photographs. Such factors were introduced to make them better represent forensic sketches in real world. This attribute is one of the main reasons for performance loss of most face sketch synthesis algorithms. That comparative work computed values of SSIM and face-recognition scores by NLDA [41] technique. There, we see that Fast-RSLCR achieved best scores against other methods and its performance gap is much smaller to FCN which scored as second-best. We reprint a portion of that result as ‘existing work’ in our results section here to compare with the results of our work. It is also obvious from these scores that Fast-RSLCR and FCN are valid candidates for further improvement regarding CUFSF or any other dataset that offers more diversity than CUFS. Lastly, we see from these results that all methodologies’ scores are in 70’s and below regarding CUFSF dataset whereas their results lie in 90’s when applied to the CUFS dataset. It is compelling evidence that:

- (i) Given methodologies are unable to handle a diversity of face images.
- (ii) They need further improvement of respective algorithms and reconsideration of process details.
- (iii) A new scheme may be devised to collectively utilize the merits of given methods for CUFSF or any other dataset containing variations as discussed earlier.

3. Proposed methodology

In the previous section, we discussed individual techniques of face-sketch generation/synthesis work well on the dataset with the least diversity of ethnicity, facial features, and age. Their performance is less in comparison to a dataset like CUFSF which does contain said variation. Moreover, we have also observed that FCN [36] and Fast-RSLCR [39] are two techniques that qualify for improvement. The novelty of our work lies in the effort by which we propose the parallel fusion of these two techniques whereby ‘synthesis’ properties of Fast-

RSLCR and ‘generative’ characteristics of FCN are combined to yield a sketch which is devoid of inherent shortcomings of individual techniques, and it also contains the benefits of parent methodologies such as:

- (a) The shapes and contours become sharp.
- (b) Edges of the sketch do not contain any deformations.
- (c) Collectively the sketch is a reliable map of variation of facial features in the dataset.

A. Methodologies Considered for Fusion.

The main objective of the combining phase is to capture significant features from the candidate sketches and combine them into one unit by preserving their characteristic details. This process must not omit or lose any high-frequency component of the candidate sketches to retain the sharpness of the facial features and their contours. Therefore, we selected the following techniques of image fusion for their respective merits. Our proposed setup is explained in Fig. 1.

3.1. Fcn

The Fully Convolutional Network [36] consists of six layers. It gets an input image of size 200x155. Two extra channels X and Y are added to already three channels RGB of the photo.

Rectified linear units are used as the activation functions. While moving through the layers of the respective size shown on each layer, a pseudo sketch is ‘generated’, and its size is cropped to 188x143 to avoid the border effect. We further process these sketches during our fusion methods which are discussed in subsequent text.

3.2. Rslcr

Random Sampling and Locality Constraint [39] takes a complete set of training photos and corresponding viewed-sketches. They are divided into an equally sized mesh of patches that are randomly selected in an offline manner and their relationship is recorded. For a testing photo, the candidate patches are selected based on locality constraint and PCA. These selected patches are then assembled into a pseudo sketch which is further processed in our union techniques as discussed here next. We used the Fast-RSLCR version of this methodology.

B. Fusion Approaches.

Three fusion methodologies are considered to test performance of the proposed system. These approaches are discussed in the accompanying section.

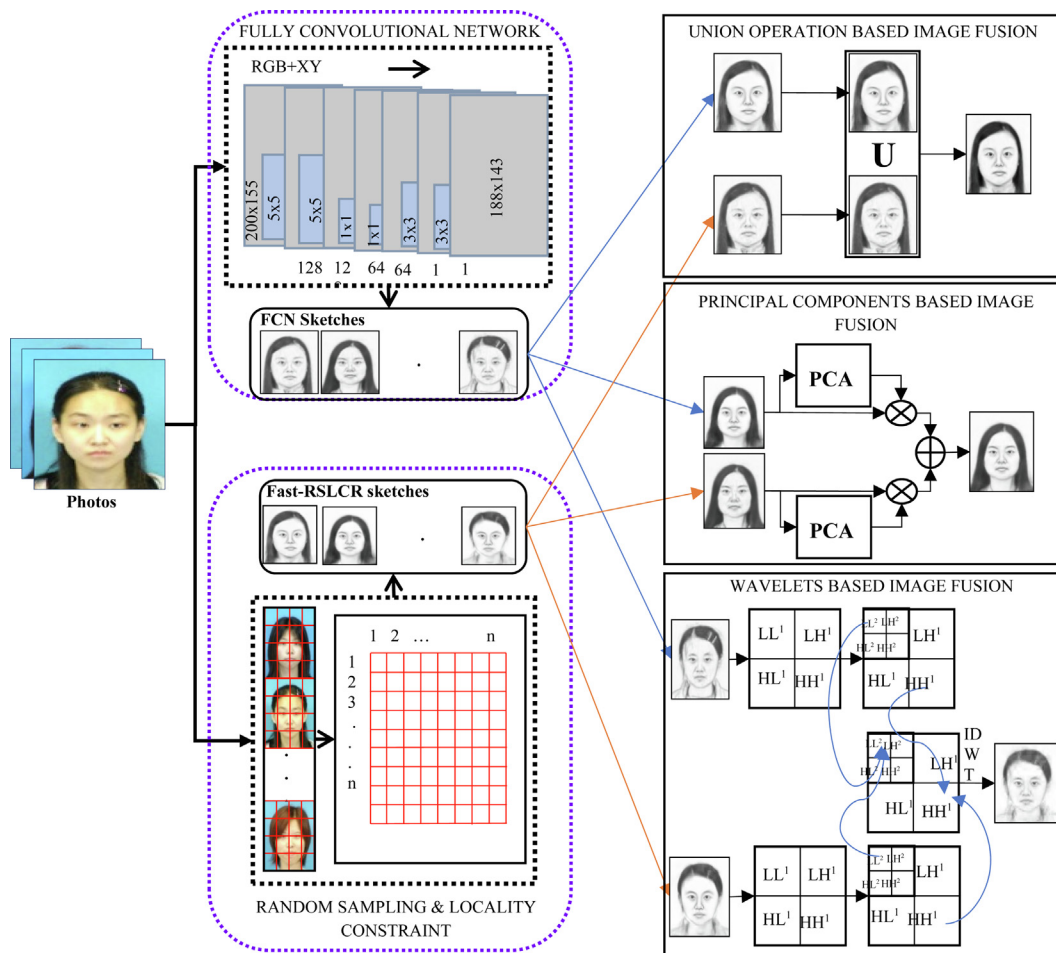


Fig. 1 Process diagram of the proposed setup.

3.3. Simple union by arithmetic approximation

In this methodology, focus is on pixel intensity and the general texture of the two sketches. We carry out a fusion of sketches by attributing pixel intensities of two images to each color channel of the resulting image which is finally approximated to grayscale value. The relationship is expressed in Equation (1). X, Y are any two images of identical size (m*n) pixels, and I is the resulting unified sketch. Given images are first rescaled to a common mask which roughly aligns the eyes, noses, and other facial features. It's done with the help of a rectangle aligned at the center of the image. Then their pixel intensities are normalized considering a minimum as 0 and maximum as 1.

$$I(m, n) = [(X_{ij} \cap Y_{ij}), (X_{ij} \cap Y_{ij}), (X_{ij} \cap Y_{ij})]_{i=1 \rightarrow m}^{j=1 \rightarrow n} \quad (1)$$

$$I \neq [(X, X, X), \dots \text{and} \dots I \neq [(Y, Y, Y)]$$

In Equation (1), I (m.n) is the resulting unified sketch. X is the first candidate sketch and Y is the second candidate sketch. i and j are the instantaneous values, and they are sequentially selected from 1 to m and from 1 to n respectively. The \cap sign indicates that either X or Y pixel is selected according to the preset condition. Three repetitions of $(X_{ij} \cap Y_{ij})$ indicate that these are the three pseudo RGB channels of resulting RGB sketch. The condition expressed in second line of the equation stipulates that I am resulting unified sketch cannot be composed of all its three pseudo RGB channels being equal to pixel intensities of either X or Y sketches. At least one channel must be different when the other two channels are identical. It is further explained in Algorithm 1.

The procedure starts by formulating an empty RGB image. We nominate or manually preset values of r, s, and t as either 1 or 2 where 1 stands for the first input sketch and 2 relates to the second input sketch.

Let's assume we set options to $(r, s, t) = (2, 1, 2)$. We award channel 1 and channel 3-pixel values of the second sketch and channel 2 gets intensity values of the first sketch. This selection procedure is arbitrary, and it can depend upon following factors of component sketches concerning the original photo:

- a) Image quality values like SSIM, FSIM, etc.
- b) Visual aesthetic integrity (resemblance, completeness, less-noise, no-extra-artifacts) determined by subjective assessment.
- c) Hit-n-trial experimentation of the component sketches.

The result is an intermediate RGB structure. It is converted to a grayscale format. The resulting image is a unified sketch that contains the contribution of intensity at every pixel from two-component sketches. Therefore, its composition is enhanced as compared to the individual sketches before fusion. The detail is given in Algorithm 1. An example is given by illustrations in Table 1.

Algorithm 1 Simple Union by arithmetic approximation

Input: Images X, Y

Step 1: $X' \leftarrow$ Convert to grayscale X
 $Y' \leftarrow$ Convert to grayscale Y

Step 2: Select options (r, s, t) where $r, s, t \in (1, 2)$

1 award 1st Image & 2 awards 2nd image to respective R, G, B channels

Restriction: options $\neq (1, 1, 1)$ and options $\neq (2, 2, 2)$

Step 3: Formulate RGB image 'Result'
 $Result \leftarrow (X'^r Y'^s, X'^r Y'^s, X'^r Y'^s)$







according to options (r, s, t)

Step 4: $I \leftarrow$ convert to grayscale (Result)

Output: Fused Image I

Table 1 Illustration of simple union by arithmetic approximation.

| Steps | 1st Sketch | 2nd Sketch |
|--|---|---|
| Input Images |  |  |
| Convert to Grayscale |  |  |
| Manually Select Values of r, s, and t | Let $r = 2, s = 1, t = 1$ options = $(2, 1, 1)$ | |
| Formulate 'Result' by awarding input sketches to a respective channel according to options (r, s, t) | Channels | R, G, B |
| | Options | 2, 1, 1 |
| | Award sketches |  |
| Convert 'Result' to grayscale to get fused image I |  | |

| Steps | | 1 st Sketch | 2 nd Sketch |
|---|----------------|--|---|
| Input Images | |  |  |
| Convert to Grayscale | |  |  |
| Manually Select Values of $r, s,$ and t | | Let $r = 2, s = 1, t = 1$ $\therefore options = (2, 1, 1)$ | |
| Formulate 'Result' by awarding input sketches to a respective channel according to <i>options</i> (r, s, t) | Channels | R, G, B | |
| | Options | $2, 1, 1$ | |
| | Award sketches |  | |
| Convert 'Result' to grayscale to get fused image I | |  | |









| Original Face Image | Synthesized Sketches | | |
|---|---|--|---|
| | Fast-RSLCR | FCN | SIMPLE_U |
|  |  |  |  |
|  |  |  |  |

Fig. 2 Effect of Simple union technique.

In Fig. 2, the positive effect of the Simple Union technique is further highlighted by candidate images from two datasets.

3.4. Principal components-based image fusion

We combine two sketches with the help of respective weights calculated upon Principal Component Analysis [42–44] of two sketches as expressed in [45]. The relationship is given in Equation (2). X and Y are any two sketches of identical size ($m \times n$) pixels. Then unified sketch I (m, n) is given by:

$$I(m, n) = \sum_{i,j=1}^{m,n} \{PCA_X * X_{ij}, PCA_Y * Y_{ij}\} \quad (2)$$

In Eq (2), different symbols are:

$I(m, n)$: the final unified image.

PCA_X and PCA_Y : respective weighting values based on its principal component calculations from X and Y matrices.

X_{ij} and Y_{ij} : individual pixel intensities at the i^{th} row and j^{th} column of respective X and Y matrices.

In Equation (2) $I(m, n)$ is the resulting unified sketch. The values of PCA lie between 0 and 1. Each pixel intensity of the unified sketch is equal to sum of corresponding pixels of X and Y multiplied by their respective values of PCA. Therefore, each pixel of the unified sketch is a PCA-weighted sum of corresponding values of X and Y .

First, covariance matrix C of the input sketches is computed. Then we calculate the matrix of full Eigenvalues V and diagonal vector D of Eigenvalues based on the covariance matrix C . Their relationship is given by:

$$C * V = V * D \quad (3)$$

PCA is then determined by a magnitude comparison of two diagonal values in D . Depending upon the outcome of the comparison, either column of V is normalized, and its two values are awarded to two entries of the PCA vector. Finally, the addition of two input images weighted by scalar multiplication with a respective column of the PCA matrix gives the unified sketch. The detail is presented in Algorithm 2.

Algorithm 2 Principal Components Based Image Fusion

Input: Images X, Y

Step 1: $C \leftarrow$ Co-Variance (X, Y)

Step 2: [Eig_vector, Eig_diag] \leftarrow Eigen Transform (C)

Step 3: if $Eig_diag(1,1) > Eig_diag(2,2)$

$PCA \leftarrow$ mean [Eig_vector (first_column)]

else

$PCA \leftarrow$ mean [Eig_vector (second_column)]

Step 4: $I \leftarrow$ sum ($PCA(1) * X, PCA(2) * Y$) || Image fusion

Output: Unified Image I

In Fig. 3, the positive effect of PCA based fusion technique is further highlighted by two candidate images from two datasets.

3.5. Wavelets based image fusion

The third technique of fusion of sketches belongs to the wavelet domain. We applied the wavelet algorithm as expressed in

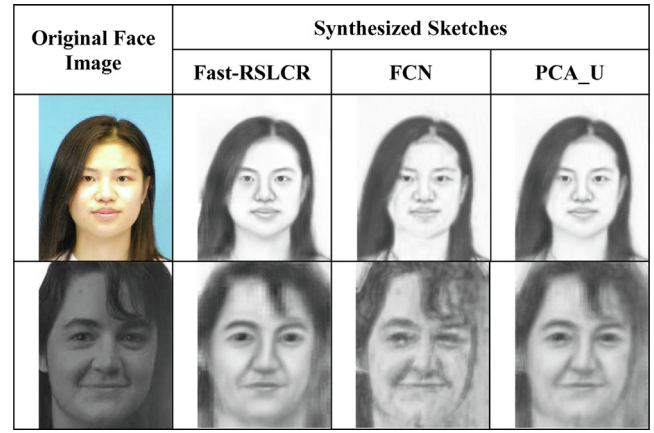


Fig. 3 Effect of PCA Fusion technique.

[46] and [47]. It decomposes the given image into wavelet coefficients according to second-order Daubechies wavelet known as dB2 [48]. We selected this wavelet since it is arbitrary regular and its compact support for orthogonal analysis exists. Moreover, its scaling function is available, and the exact reconstruction of the signals/images is possible after their decomposition and subsequent fusion. This wavelet bears the properties of both discrete and continuous transformation which help in signal analysis and compression. Lastly, Daubechies wavelets (DBN) can be computed with a fast algorithm. N denotes the order of the wavelet.

Explicit expressions for wavelets of this class do not exist, except for dB1. Instead, they can be represented by the squared modulus of the transfer function of their associated filter f [49]. Let $\sum_{j=0}^{N-1} C_{N-1}^j$ be the binomial coefficients then.

$$H_0(\omega) = \frac{1}{\sqrt{2}} \sum_{j=0}^{N-1} f_j e^{-ij\omega} \quad (4)$$

$$B(y) = \sum_{j=0}^{N-1} C_{N-1}^j + y^j \quad (5)$$

$$|H_0(\omega)|^2 = \{(\cos^2(\frac{\omega}{2}))^N B\{\sin^2(\frac{\omega}{2})\}\} \quad (6)$$

Equation (4) mentions the associated filter f and its transform H , Equation (5) presents related coefficients and Equation (6) contains the defining relationship of Daubechies wavelets. In these equations y is the signal variable, ω is the frequency, and N is the order of wavelet as in the case of DBN . Three factors play an important role while combining two sketches by this scheme. The first factor is the level of decomposition of the image. We chose level 5 which retains a fair degree of original information of the image properties.

The second and third factors relate to the methods of selecting ‘approximations’ and ‘details’ while combining two images. They may be any of the *minimum*, *maximum*, *mean*, *image-1*, *image-2*, or a *random* value. Four combinations were tried namely, max-max, max-min, mean-mean, and min-max. These factors are further discussed in [48,49]. In Fig. 4, the effect of the Wavelet-based Union technique is shown by two candidate images from two datasets. The scheme of this fusion method is given in algorithm 3.

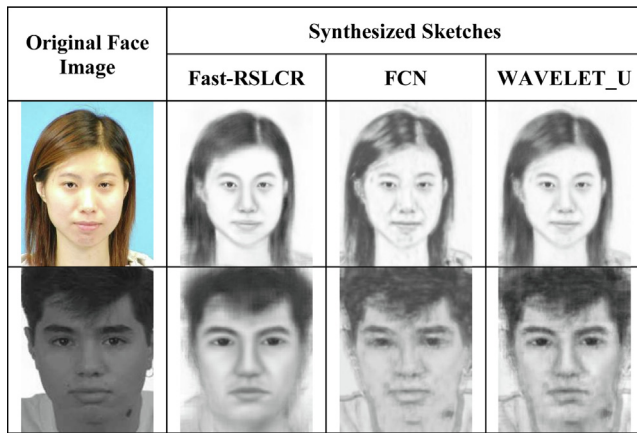


Fig. 4 Effect of Wavelet Union technique.

Algorithm 3 Wavelets Based Image Fusion

Input: Images X, Y , Wavelet Name w_name , Level l , Approximation a , Detail d
 Step 1: $X' \leftarrow \text{Wavelet Decompose}(X, l, w_name)$
 Step 2: $Y' \leftarrow \text{Wavelet Decompose}(Y, l, w_name)$
 Step 3: $\text{Unified Co_Effs} \leftarrow \text{Wavelet Fusion}(X', Y', a, d)$
 Step 4: $I \leftarrow \text{Wavelet Reconstruction}(\text{Unified Co_Effs})$
Output: Fused Image I

4. Experiments and results

We conducted our experiments through MatLab R2017a running on Core i5® CPU 5400, @2.66 GHz, 4 GB physical memory, and 64-bit operating system. Practical implementation involved the fusion of images by Simple, PCA, and Wavelet methods. The third method further included four cycles of computations for min-max, max-min, max-max, and mean-mean options. dB2 wavelet and level 5 of the decomposition were used. Some sample sketch images formed by the proposed and existing methods are illustrated in Fig. 5.

A. Datasets

Experiments were conducted on two publicly available datasets. First is named CUFS and it is an acronym for the Chinese University of Hong Kong (CUHK) Face Sketch database [17] and it is further composed of three other datasets. Those components are shown in Table 2. The second dataset is called CUFSF [17] which is based on 1194 images selected by the academics of CUHK from photo-sketch pairs of FERET database [50]. Authors of [18] implemented different algorithms from state of the art. Sketches produced by their work are publicly available for further academic research. We used the set of resulting synthesized sketches (338 from CUFS and 944 from CUFSF) for our fusion studies. It may be noted that the total numbers of images (606 of CUFS and 1194 of CUFSF) do not apply to our work. Further configuration of these datasets is given in Table 2.

B. Performance Measures.

The performance measures used in this work are discussed in the accompanying subsections.

4.1. Ssim

Structural SIMilarity Index (SSIM) [53] is a legacy parameter to ascertain similarity of the individual and unified sketches to their respective viewed-sketches. It was put forth by Wang et al [53]. We use this parameter here to undertake a comparison of our results with previous works in the state of art.

We computed all evaluation parameters to gauge the quality of unified sketches concerning their gold standard of viewed sketches drawn by the artists. Since each of FCN [36] and Fast-RSLCR [39] used pairs of original photos and viewed-sketches as a training medium, therefore at this stage SSIM gives us a clear estimation of how much the proposed methodology has effectively imitated, reproduced and/or restored descriptive properties of the sketch artists. SSIM values were computed in two arrangements. SSIM value was computed between a synthesized-sketch and its corresponding forensic-sketch, and we documented it as '*concerning sketches*'. This type is recorded simply as SSIM in previous works. Secondly, we calculated SSIM value between a synthesized-sketch and its corresponding photo (grayscale) and we termed it as '*concerning photos*'. Equation (7) shows mathematical relationship of SSIM. It is reproduced here from [53]. SSIM value equal to -1 signifies completely isolated inputs and its value equal to $+1$ depicts truly identical images. Tables 3 and 4 show SSIM values calculated for discrete datasets for their comparison with component techniques of the fusion operation.

$$SSIM(X, Y) = \frac{(2h_X h_Y + K_1)(2Z_{XY} + K_2)}{(h_X^2 + h_Y^2 + K_1)(Z_X^2 + Z_Y^2 + K_2)} \quad (7)$$

where.

X, Y = image signals.

h = mean intensity.

Z = variance, equal to the square root of standard deviation.

K_1, K_2 = constants.

4.2. Nlda

Our primary focus is an attempt to test image fusion to improve the quality of synthesized- sketches by two different methodologies. Therefore, the choice of any reliable algorithm to run face-recognition step as validation parameter would suffice. Therefore, to test the efficacy of our proposed methodology we chose Nullspace Linear Discriminant Analysis (NLDA) process [41]. This technique is also employed by other works like [18,36,39 54535352] regarding face-sketch synthesis. With this scheme, we were able to compare our results with state of the art. The software code of this technique was reused from [55].

C. Evaluation Protocol

Experimentation was conducted in two phases according to the first and second datasets. In each phase, average SSIM scores were measured for unified sketches in contrast to their viewed sketches. We included synthesized sketches of FCN, Fast-RSLCR and our experimentation to compute SSIM

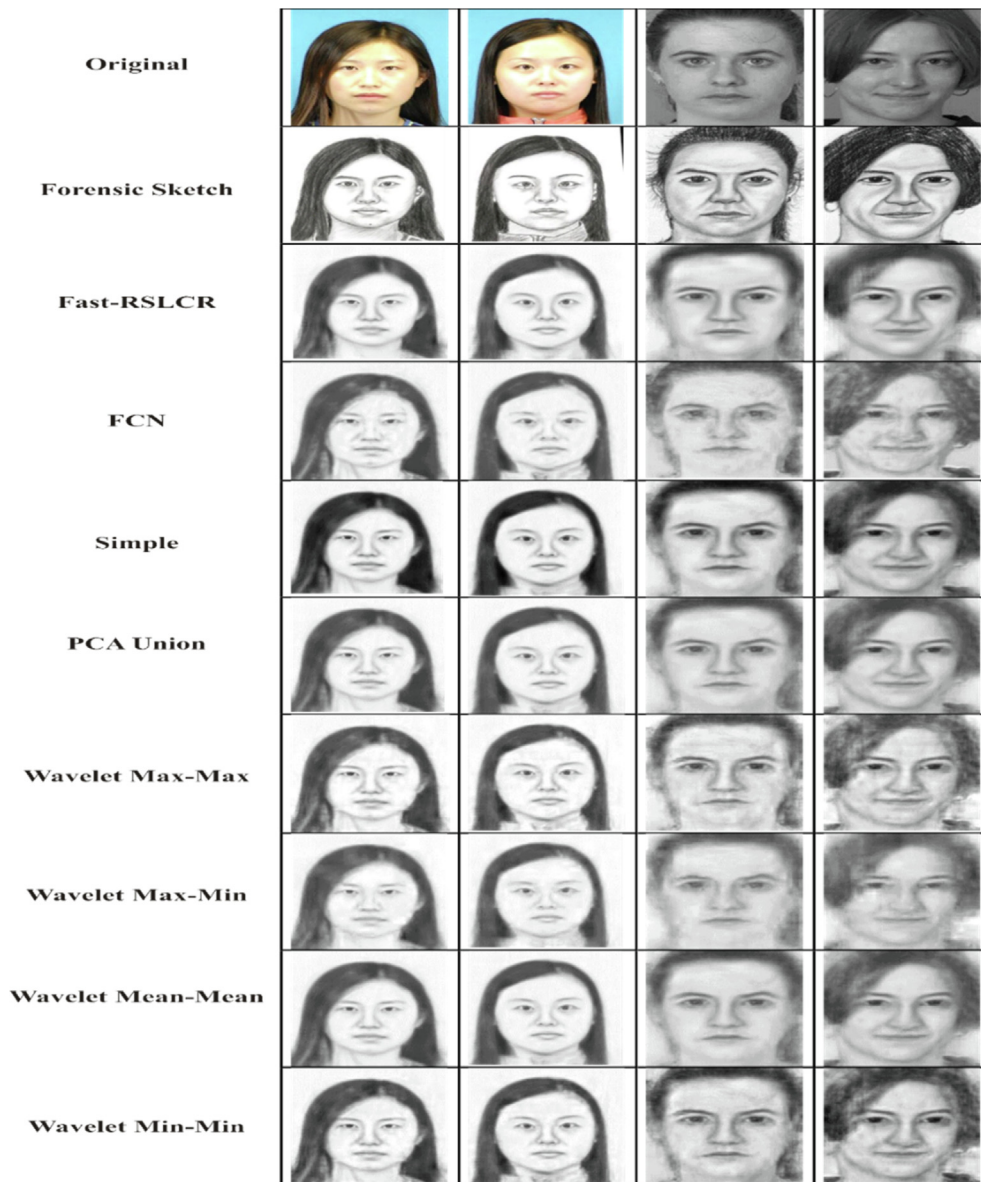


Fig. 5 Comparison of sketches by individual and fusion methods.

Table 2 Details of datasets For face-recognition procedure.

| EXISTING WORK | | | |
|---------------|-------|----------|---------|
| Name | Total | Training | Testing |
| CUFS[17] | 606 | 268 | 338 |
| CUHK[17] | 188 | 80 | 100 |
| AR[51] | 123 | 80 | 43 |
| XM2VTS[52] | 295 | 100 | 195 |
| CUFSF[17] | 1194 | 250 | 944 |
| Feret[50] | 1194 | 250 | 994 |
| PROPOSED WORK | | | |
| CUFS [18] | 338 | 150 | 188 |
| CUFSF [18] | 944 | 300 | 644 |

and face-recognition scores under identical conditions and protocol. The pattern of training and testing splits for NLDA was also similar for all techniques during calculations. Our

experimentation revealed slightly superior scores for these two methods (FCN and Fast-RSLCR) as compared to their published results in corresponding papers.

We ran the NLDA [41] sequence for each of our six proposed procedures by using image- unified sketches pairs as training medium and unified sketches as testing elements. Our setup considered 149 features for the CUFS dataset and 299 features for the CUFSF dataset while computing face recognition rates for each of our proposed six methodologies. These features are the number of dimensions of each sketch-image that are considered iteratively during the NLDA procedure. Moreover, a higher number of features for CUFSF versus CUFS datasets were considered due to more complexity of the former database. In the first experiment, CUFS [18] dataset was employed comprising 338 unified sketches. Serial numbers of 150 sketches were randomly selected and their corresponding original viewed sketches were used to train the NLDA model. The remaining 188 unified sketches were employed in

Table 3 Mean values of SSIM (%) for CUFS [18] dataset.

| Methods | EXISTING TECHNIQUE | | PROPOSED TECHNIQUES | | | | | |
|--------------------------|--------------------|----------|---------------------|------------|----------------------|---------|-----------|---------|
| | Fast-RSLCR [39] | FCN [36] | Simple Union | PCA Fusion | Wavelet-Based Fusion | | | |
| | | | | | Max-Max | Max-Min | Mean-Mean | Min-Max |
| With respect to Sketches | 55.42 | 52.14 | 54.23 | 54.70 | 53.17 | 53.40 | 54.60 | 52.77 |
| With respect to Photos | 53.26 | 54.28 | 56.70 | 55.01 | 52.56 | 52.44 | 55.04 | 53.32 |

Table 4 Success rates (%) for face recognition on CUFS [18] dataset at 1/3rd of features against FCN.

| | EXISTING TECHNIQUE | | PROPOSED TECHNIQUES | | | | |
|--------------|--------------------|------------|---------------------|------------|----------------------|------------|-----------|
| | FCN [36] | | Simple Union | PCA Fusion | Wavelet-Based Fusion | | |
| | | | | | Max-Max | Max-Min | Mean-Mean |
| SUCCESS RATE | 96.49 % | 96.46 % | 96.49 % | 96.49 % | 96.53 % | 96.52 % | 96.54 |
| FEATURES | 94 | 32 | 30 | 30 | 44 | 31 | 44 |
| TIME | 265.3 msec | 105.8 msec | 106.2 msec | 106.2 msec | 124.4 msec | 109.7 msec | 124.4 |

the testing phase. Twenty such iterations were carried out and face recognition accuracy viz a viz number of features at which this rate was registered were recorded. In the second experiment, we focused on CUFSF [18] comprising 944 unified sketches. Serial numbers of 300 unified images and their corresponding original photo – viewed sketch pairs trained the NLDA model. Rest 644 fusion sketches were employed in the testing phase. As before, twenty iterations of this process were conducted, and face recognition accuracy and the relevant number of features where that recognition accuracy was achieved, were recorded. Then these rates were sequentially compared to similar results of individual techniques FCN and Fast-RSLCR. These comparisons, their graphical representations, and short discussions are presented in the next sub-section. It may be noted that results of this experimentation are compared with the individual constituent techniques only and they are not compared with other methods in state of the art. It is an endeavor of this work to test and validate that fusion of sketches from component methods can yield images of superior quality than the original parts. Moreover, in following sections D. and E. improvements achieved by fusion techniques over the component methodologies are highlighted with the help of discussion text, tables, and graphs about evaluation parameters like SSIM and face recognition scores.

D. Results on CUFS dataset

Results for SSIM in Table 3 indicate that the fusion of sketches performs at par the individual approaches on CUFS [18] dataset.

It signifies the possibility that most images of CUFS did not contain much diversity and therefore individual techniques were already able to mimic optimum features of the sketch artists from their sketches. Fig. 6 plots Cumulative Frequency Distribution of different techniques for SSIM scores.

It is observed that most sketches by Fast-RSLCR [39] and FCN [36] lie in values 0.65 and below. After this region, the Fast-RSLCR graph/line of CDF drops sharply. On the con-

trary, a small area under the curve of Fusion techniques lies in this region. A major chunk of their values spans a mid-region of 0.5 to 0.7 SSIM score whereas less than 10% of sketches by Fast-RSLCR [39] and FCN [36] could achieve this score. The efficacy of fusion techniques is then highlighted by results of face recognition given in Tables 4 and 5. These tables highlight success rates of recognition as % age, the number of features at which that score was attained is given as a number in the next lower row and the third row in each set contains computational time taken by each technique to register that accuracy rate. Table 4 gives the original score of the FCN [36] technique compared with the success rates achieved by our proposed methodologies. Table 5 shows the results of our proposed techniques compared to the existing algorithm of Fast-RSLCR [45]. All of the fusion techniques achieved similar rates of accuracy at 1/3rd of features against FCN [36] and almost 2/3rd of features versus Fast-RSLCR [39]. This factor translates into saving computational costs by the same ratio (around one-third against FCN [36] and almost two-third versus Fast-RSLCR [45]) regarding the search for a correct face match. Fig. 7 shows a combined plot of the success rates for face recognition routine by existing and proposed techniques on CUFS [45] dataset.

E. Results on CUFSF dataset

SSIM scores in Table 6 for CUFSF [48] dataset show that proposed methods for fusion of sketches perform superior to the individual approach FCN [36] and at par with Fast-RSLCR [39].

Fig. 8 highlights the comparison and improved values of SSIM scores for existing and proposed methodologies. Performance jump by almost 5 points in SSIM values validates the assumption that individual techniques do not fully capture descriptive features of the viewed sketches when they involve a diversity of race, age, and ethnicity which occur more in the CUFSF dataset than the CUFS database.

This assertion is further validated by comparison of success rates of face recognition routine by NLDA as given in Tables

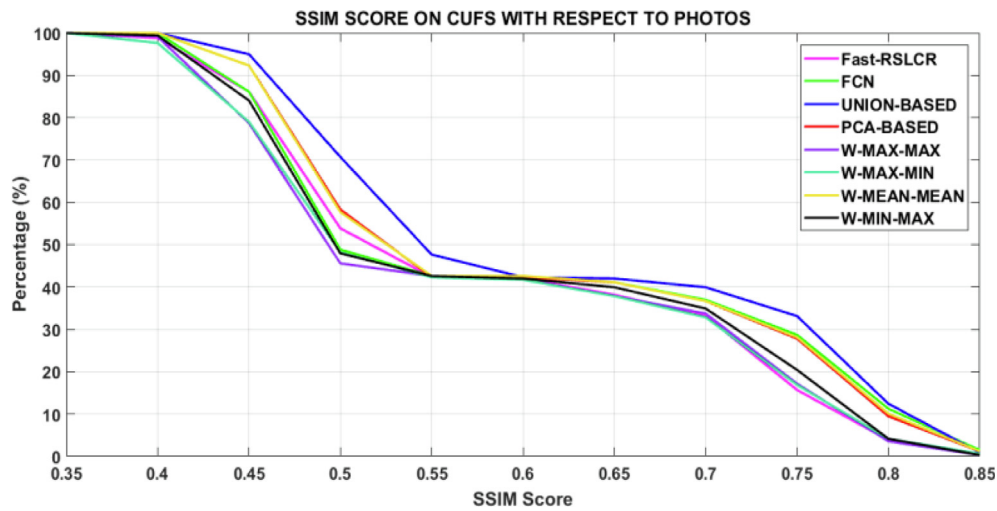


Fig. 6 SSIM scores of Fast-RSLCR [39], FCN [36] and proposed techniques on CUFS [18] dataset.

Table 5 Success rates (%) for face recognition on CUFS [18] dataset at 2/3rd of features versus Fast-RSLCR.

| | EXISTING TECHNIQUE | PROPOSED TECHNIQUES | | | | | |
|--------------|--------------------|---------------------|------------|----------------------|------------|------------|------------|
| | | Simple Union | PCA Fusion | Wavelet-Based Fusion | | | |
| | Fast-RSLCR [39] | | | Max-Max | Max-Min | Mean-Mean | Min-Max |
| SUCCESS RATE | 98.43 % | 98.01 % | 98.27 | 98.01 % | 98.01 | 98.01 | 98.01 % |
| FEATURES | 124 | 97 | 83 | 94 | 90 | 94 | 90 |
| TIME | 287.8 msec | 225.5 msec | 205.5 msec | 214.5 msec | 217.9 msec | 214.5 msec | 207.1 msec |

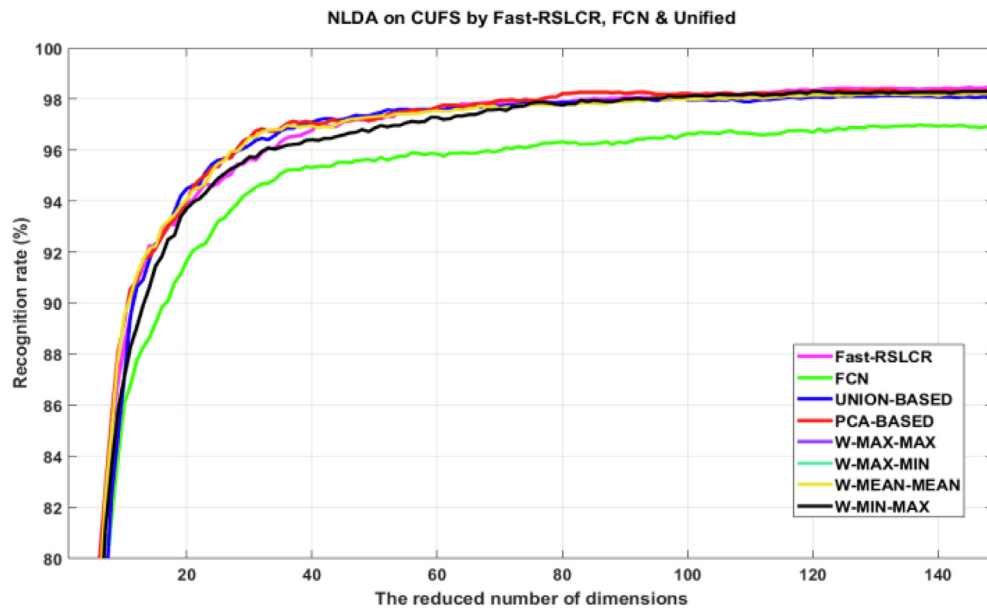


Fig. 7 NLDA Face recognition accuracies of Fast-RSLCR [39], FCN [36], and proposed techniques on CUFS [18] dataset.

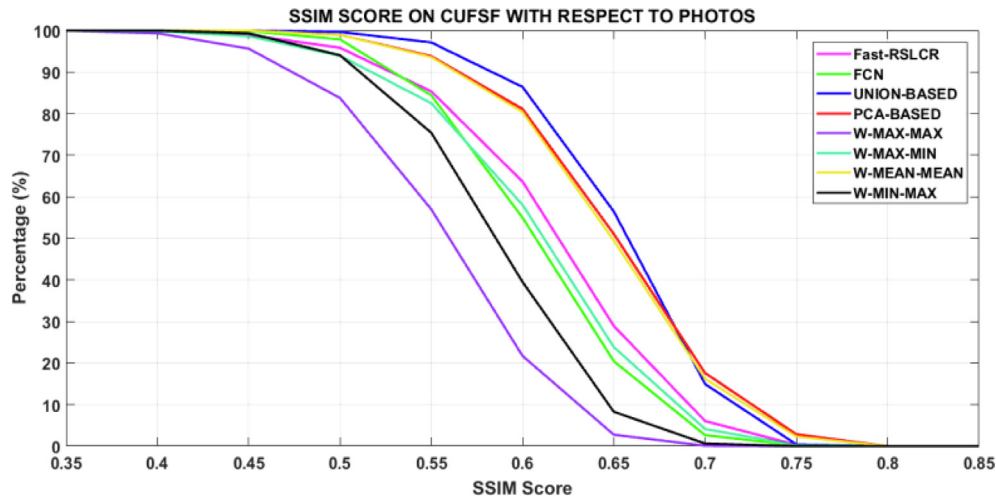
7, 8, and 9. Table 7 contains comparison scores of existing method FCN [36] and our proposed techniques. All of the fusion techniques achieved similar and improved rates of accuracy versus FCN [36]. Simple Union and PCA Fusion methods

gained the same accuracy as FCN [18] at almost 1/3rd features and at 1/2 or lesser computational time.

Tables 8 and 9 respectively show a comparison of success rates for the existing method Fast-RSLCR [39] and the pro-

Table 6 Mean values of SSIM (%) for CUFSF [18] dataset.

| Methods | Existing Work | | Proposed Work | | | | | |
|--------------------------|-----------------|----------|---------------|------------|---------|---------|-----------|---------|
| | Fast-RSLCR [39] | FCN [36] | Simple Union | PCA Fusion | Wavelet | | | |
| | | | | | Max-Max | Max-Min | Mean-Mean | Min-Max |
| With respect to Sketches | 44.56 | 36.22 | 41.97 | 42.60 | 39.55 | 39.31 | 42.02 | 39.71 |
| With respect to Photos | 56.45 | 55.53 | 60.29 | 59.69 | 50.56 | 55.49 | 59.51 | 53.37 |

**Fig. 8** SSIM scores of Fast-RSLCR [39], FCN [36] and proposed techniques on CUFSF [45] dataset.**Table 7** Mean values of success rates (%) for face recognition on CUFSF [18] dataset.

| | EXISTING TECHNIQUE | PROPOSED TECHNIQUES | | | | | |
|--------------|--------------------|---------------------|-------------------|---------------------------------|------------|------------|------------|
| | FCN [36] | Simple Union | PCA Fusion | <i>FUSION IN WAVELET DOMAIN</i> | | | |
| | | | | Max-Max | Max-Min | Mean-Mean | Min-Max |
| SUCCESS RATE | 69.43 % | 70.18 % | 70.14 % | 69.48 % | 69.5 % | 69.48 % | 69.5 % |
| FEATURES | 114 | 43 | 40 | 57 | 71 | 57 | 71 |
| TIME | 643.8 msec | 327.5 msec | 295.7 msec | 371.8 msec | 437.7 msec | 371.8 msec | 437.7 msec |

Table 8 Mean values of success rates (%) for face recognition on CUFSF [18] dataset, comparison of proposed methods with 1st reference value of existing method.

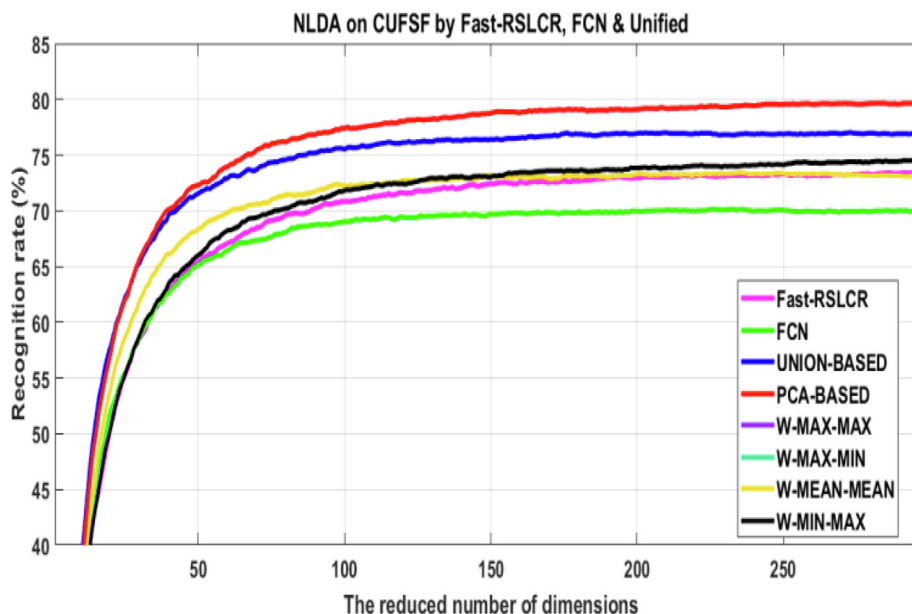
| | EXISTING TECHNIQUE | PROPOSED TECHNIQUES | | | | | |
|--------------|--------------------|---------------------|-------------------|---------------------------------|------------|------------|------------|
| | Fast-RSLCR [39] | Simple Union | PCA Fusion | <i>FUSION IN WAVELET DOMAIN</i> | | | |
| | | | | Max-Max | Max-Min | Mean-Mean | Min-Max |
| SUCCESS RATE | 73.16 % | 73.70 % | 73.50 % | 73.12 % | 73.02 | 72.38 % | 73.02 % |
| FEATURES | 216 | 67 | 57 | 148 | 136 | 97 | 136 |
| TIME | 1110.4 msec | 432.6 msec | 367.8 msec | 734.1 msec | 687.6 msec | 659.8 msec | 687.6 msec |

posed algorithms. In Table 8 it is depicted that competing values for both domains. It indicates the time-efficient performance of our proposed techniques at par with the most

optimum value of Fast-RSLCR [39]. It is observed that more importantly, Simple and PCA Fusion techniques achieved slightly higher recognition rates at **67** and **57** features respec-

Table 9 Mean values of success rates (%) for face recognition on CUFSF [18] dataset, comparison of proposed methods with highest reference value of existing method.

| | EXISTING TECHNIQUE | PROPOSED TECHNIQUES | | | | | |
|--------------|--------------------|---------------------|-------------------|---------------------------------|-------------|------------|-----------|
| | | Simple Union | PCA Fusion | <i>FUSION IN WAVELET DOMAIN</i> | | | |
| | Fast-RSLCR [39] | | | Max-Max | Max-Min | Mean-Mean | Min-Max |
| SUCCESS RATE | 73.41 % | 76.11 % | 79.03 % | 73.39 % | 74.09% | 73.19 % | 74.03 % |
| FEATURES | 286 | 121 | 167 | 235 | 222 | 149 | 219 |
| TIME | 1402.7 msec | 634.4 msec | 846.6 msec | 1195 msec | 1121.2 msec | 755.1 msec | 1138 msec |

**Fig. 9** NLDA Face recognition accuracies of Fast-RSLCR [39], FCN [36] and proposed techniques on CUFSF [45] dataset.

tively than Fast-RSLCR [39] which exhibited the same value at 286 features out of a total 299 dimensions in the first set. This translated to three times improvement in computational costs. Table 9 highlights the improved performance of our methods against the highest score of Fast-RSLCR [39]. Here too, the Simple Union technique registered a performance jump of 2.7% by employing only 121 features whereas the PCA Fusion method showed an improvement of 5.62% by employing 50 features less than the highest score of Fast-RSLCR [39]. It also established the fact that fusion techniques address inadequacies of individual sketches and impart them robust features, clarity and sharp contours which aid in the face recognition process. With the help of face recognition routine by the NLDA algorithm, we measured the performance of different schemes of face sketch synthesis (see Fig. 9).

In comparison to individual techniques, we observe in Tables 7 to 9 that on both datasets different versions of unified sketches achieve similar values of scores at far fewer features with better computational efficiency. It augments the proposed idea that by fusion of two sketches that have certain merits as well as inadequacies, we achieved a unified sketch containing strong features.

5. Conclusion

It is proved that SSIM scores of FCN and Fast-RSLCR techniques improve when their resulting sketches are unified by different merging techniques. Best achieved SSIM score was 60.29 which is 3.84 points better than Fast-RSLCR and 4.76 points higher than FCN regarding the CUFSF dataset. Proposed methodology at best achieved 68% improvement (30 vs 94) over FCN and 33% improvement (83 vs 124) over Fast-RSLCR concerning a lesser number of features for detection regarding CUFS. For the CUFS dataset, Simple Union and PCA fusion methods worked better. The proposed scheme achieved similar detection rate at 73% lesser features (57 vs 216) and 5.62% higher detection rate at 41% less features (167 vs 286) concerning Fast-RSLCR regarding CUFSF dataset For CUFSF dataset Simple Union and PCA fusion methods showed enhanced results and Wavelet Mean-Mean methodology showed competitive performance within Wavelet Fusion domain. The chief characteristics of our proposed methodologies by merging strong features of the candidate sketches proved to be useful against the weak properties of either sketch. Overall, the proposed setup achieved three times

(367.8 msec vs 1110.4 msec) better computational performance versus the individual methods.

Declaration of Competing Interest

The authors declare that they have no known competing financial interests or personal relationships that could have appeared to influence the work reported in this paper.

Acknowledgements

This study was supported by the BK21 FOUR program (Education and Research Center for Securing Cyber-Physical Space) through the National Research Foundation (NRF) funded by the Ministry of Education of Korea (5199990314137).

References

- [1] S.L. Fernandes, G.J. Bala, ODDROID XU4 based implementation of decision level fusion approach for matching computer generated sketches, *J. Comput. Sci.* 16 (2016) 217–224.
- [2] S.L. Fernandes, G.J. Bala, Self-Similarity Descriptor and Local Descriptor-Based Composite Sketch Matching, in: *Proceedings of Fifth International Conference on Soft Computing for Problem Solving*, 2016, pp. 643–649.
- [3] S.L. Fernandes, G.J. Bala, Developing a novel technique to match composite sketches with images captured by unmanned aerial vehicle, *Procedia Comput. Sci.* 78 (2016) 248–254.
- [4] S.L. Fernandes, G.J. Bala, Image Quality Assessment-Based Approach to Estimate the Age of Pencil Sketch, in: *Proceedings of Fifth International Conference on Soft Computing for Problem Solving*, 2016, pp. 633–642.
- [5] S.L. Fernandes, G.J. Bala, Matching images captured from unmanned aerial vehicle, *Int. J. Syst. Assur. Eng. Manage.* 9 (2018) 26–32.
- [6] Y. Song, L. Bao, Q. Yang, M.-H. Yang, Real-time exemplar-based face sketch synthesis, in: *European conference on computer vision*, 2014, pp. 800–813.
- [7] S.L. Fernandes, G.J. Bala, Recognize faces across multi-view videos and under varying illumination, facial expressions, *Int. J. Circuits, Syst. Sign. Process. USA* 10 (2016) 7–18.
- [8] S.L. Fernandes, J.G. Bala, Recognizing faces across age progressions and under occlusion, *Recent Patents Comput. Sci.* 9 (2016) 209–215.
- [9] S.L. Fernandes, J.G. Bala, Study on MACE Gabor filters, Gabor wavelets, DCT-neural network, hybrid spatial feature interdependence matrix, fusion techniques for face recognition, *Recent Patents Eng.* 9 (2015) 29–36.
- [10] S. Lawrence Fernandes, G. Josemin Bala, 3D and 4D face recognition: a comprehensive review, *Recent Patents Eng.* 8 (2014) 112–119.
- [11] S. Lawrence Fernandes, G. Josemin Bala, “Development and analysis of various state of the art techniques for face recognition under varying poses, *Recent Patents Eng.* 8 (2014) 143–146.
- [12] B.F. Klare, A.K. Jain, Heterogeneous face recognition using kernel prototype similarities, *IEEE Trans. Pattern Anal. Mach. Intell.* 35 (2012) 1410–1422.
- [13] S.L. Fernandes, J.G. Bala, A novel decision support for composite sketch matching using fusion of probabilistic neural network and dictionary matching, *Current Med. Imag. Rev.* 13 (2017) 176–184.
- [14] C. Wilkinson, “A review of forensic art,” *Research and Reports in Forensic Medical Science*, p. 17, 09/01 2015.
- [15] N. Wang, D. Tao, X. Gao, X. Li, J. Li, A Comprehensive Survey to Face Hallucination, *Int. J. Comput. Vision* 106 (2014/01/01 2014.) 9–30.
- [16] T. Xiaoou and W. Xiaogang, “Face sketch synthesis and recognition,” in *Proceedings Ninth IEEE International Conference on Computer Vision*, 2003, pp. 687–694 vol.1.
- [17] X. Wang, X. Tang, Face photo-sketch synthesis and recognition, *IEEE Trans. Pattern Anal. Mach. Intell.* 31 (2008) 1955–1967.
- [18] A. Akram, N. Wang, J. Li, X. Gao, A Comparative Study on Face Sketch Synthesis, *IEEE Access* 6 (2018) 37084–37093.
- [19] S. Zhang, R. Ji, AAM Based Face Sketch Synthesis, *Neural Process. Lett.* 48 (2018) 1405–1414.
- [20] A. Radman, S.A. Suandi, Robust face pseudo-sketch synthesis and recognition using morphological-arithmetic operations and HOG-PCA, *Multimedia Tools and Applications* (2018) 1–22.
- [21] J. Jiang, Y. Yu, Z. Wang, X. Liu, and J. Ma, “Graph-Regularized Locality-Constrained Joint Dictionary and Residual Learning for Face Sketch Synthesis,” *IEEE Trans Image Process*, vol. 28, pp. 628–641, Feb 2019.
- [22] M. Sharif, J. Amin, M. Raza, M. A. Anjum, H. Afzal, and S. A. Shad, “Brain tumor detection based on extreme learning,” *Neural Computing and Applications*, pp. 1–13, 2020.
- [23] J. Amin, M. Sharif, M. Yasmin, S.L. Fernandes, Big data analysis for brain tumor detection: Deep convolutional neural networks, *Future Generation Computer Systems* 87 (2018) 290–297.
- [24] M. A. Khan, T. Akram, M. Sharif, K. Javed, M. Raza, and T. Saba, “An automated system for cucumber leaf diseased spot detection and classification using improved saliency method and deep features selection,” *Multimedia Tools and Applications*, pp. 1–30, 2020.
- [25] M. Sharif, T. Akram, M. Raza, T. Saba, A. Rehman, Hand-crafted and deep convolutional neural network features fusion and selection strategy: an application to intelligent human action recognition, *Appl. Soft Comput.* 87 (2020) 105986.
- [26] J. Amin, M. Sharif, M.A. Anjum, M. Raza, S.A.C. Bukhari, Convolutional neural network with batch normalization for glioma and stroke lesion detection using MRI, *Cognit. Syst. Res.* 59 (2020) 304–311.
- [27] M.A. Khan, M.I. Sharif, M. Raza, A. Anjum, T. Saba, S.A. Shad, Skin lesion segmentation and classification: A unified framework of deep neural network features fusion and selection, *Expert Systems* (2019) e12497.
- [28] M. Fayyaz, M. Yasmin, M. Sharif, J.H. Shah, M. Raza, T. Iqbal, Person re-identification with features-based clustering and deep features, *Neural Comput. Appl.* (2019) 1–22.
- [29] M. Rashid, M.A. Khan, M. Sharif, M. Raza, M.M. Sarfraz, F. Afza, Object detection and classification: a joint selection and fusion strategy of deep convolutional neural network and SIFT point features, *Multimedia Tools and Applications* 78 (2019) 15751–15777.
- [30] J. Amin, M. Sharif, M. Raza, T. Saba, R. Sial, S.A. Shad, Brain tumor detection: a long short-term memory (LSTM)-based learning model, *Neural Comput. Appl.* (2019) 1–9.
- [31] M. Raza, M. Sharif, M. Yasmin, M.A. Khan, T. Saba, S.L. Fernandes, Appearance based pedestrians’ gender recognition by employing stacked auto encoders in deep learning, *Future Gener. Comput. Syst.* 88 (2018) 28–39.
- [32] J. Amin, M. Sharif, N. Gul, M. Raza, M.A. Anjum, M.W. Nisar, et al, Brain Tumor Detection by Using Stacked Autoencoders in Deep Learning, *J. Med. Syst.* 44 (2020) 32.
- [33] M. Zhang, N. Wang, X. Gao, Y. Li, Markov Random Neural Fields for Face Sketch Synthesis, *IJCAI* (2018) 1142–1148.
- [34] L. Jiao, S. Zhang, L. Li, F. Liu, W. Ma, A modified convolutional neural network for face sketch synthesis, *Pattern Recogn.* 76 (2018) 125–136.

- [35] S. Zhang, R. Ji, J. Hu, Y. Gao, C.-W. Lin, Robust Face Sketch Synthesis via Generative Adversarial Fusion of Priors and Parametric Sigmoid, *IJCAI* (2018) 1163–1169.
- [36] L. Zhang, L. Lin, X. Wu, S. Ding, L. Zhang, End-to-end photo-sketch generation via fully convolutional representation learning, in: in *Proceedings of the 5th ACM on International Conference on Multimedia Retrieval*, 2015, pp. 627–634.
- [37] D. Lu, Z. Chen, Q.J. Wu, X. Zhang, FCN based preprocessing for exemplar-based face sketch synthesis, *Neurocomputing* 365 (2019) 113–124.
- [38] C. Chen, W. Liu, X. Tan, and K.-Y. K. Wong, “Semi-supervised Learning for Face Sketch Synthesis in the Wild,” in *Computer Vision – ACCV 2018*, Cham, 2019, pp. 216–231.
- [39] N. Wang, X. Gao, and J. Li, “Random sampling and locality constraint for face sketch,” *arXiv preprint arXiv:1701.01911*, vol. 2, 2017.
- [40] C. Dong, C.C. Loy, K. He, X. Tang, Image Super-Resolution Using Deep Convolutional Networks, *IEEE Trans. Pattern Anal. Mach. Intell.* 38 (2016) 295–307.
- [41] L.-F. Chen, H.-Y.-M. Liao, M.-T. Ko, J.-C. Lin, G.-J. Yu, A new LDA-based face recognition system which can solve the small sample size problem, *Pattern Recogn.* 33 (2000) 1713–1726.
- [42] M. Mudrova, A. Procházka, Principal component analysis in image processing, in *Proceedings of the MATLAB Technical Computing Conference*, 2005.
- [43] P.K. Pandey, Y. Singh, S. Tripathi, Image processing using principle component analysis, *Int. J. Comput. Appl.* 15 (2011) 37–40.
- [44] A. Hladnik, Image compression and face recognition: Two image processing applications of principal component analysis, *Int. Circular Graph. Educ. Res.* 6 (2013) 56–61.
- [45] V. Naidu, J.R. Raol, Pixel-level image fusion using wavelets and principal component analysis, *Defence science journal* 58 (2008) 338–352.
- [46] H. Om, S.K. Mishra, S. Bhatnagar, A. Shukla, A.A. Tiwari, Medical Image Fusion Based on Wavelet Transform (2014).
- [47] Y. Zhou, A. Mayyas, M.A. Omar, Principal Component Analysis-Based Image Fusion Routine with Application to Automotive Stamping Split Detection, *Research in Nondestructive Evaluation* 22 (2011/03/31 2011.) 76–91.
- [48] I. Daubechies, Orthonormal bases of compactly supported wavelets, *Commun. Pure Appl. Math.* 41 (1988) 909–996.
- [49] M. Misić, Y. Misić, G. Oppenheim, J.-M. Poggi, Wavelets and their Applications, John Wiley & Sons, 2013.
- [50] P.J. Phillips, H. Moon, P. Rauss, S.A. Rizvi, The FERET evaluation methodology for face-recognition algorithms, in: in *Proceedings of IEEE Computer Society Conference on Computer Vision and Pattern Recognition*, 1997, pp. 137–143.
- [51] A. Martínez, R. Benavente, The AR face database, 1998, Computer Vision Center, Technical Report 3 (2007) 5.
- [52] K. Messer, J. Matas, J. Kittler, J. Luettin, G. Maitre, XM2VTSDB: The extended M2VTS database, in: in *Second international conference on audio and video-based biometric person authentication*, 1999, pp. 965–966.
- [53] Z. Wang, A.C. Bovik, H.R. Sheikh, E.P. Simoncelli, Image quality assessment: from error visibility to structural similarity, *IEEE Trans. Image Process.* 13 (2004) 600–612.
- [54] L. Zhang, L. Lin, X. Wu, S. Ding, and L. Zhang, “End-to-End Photo-Sketch Generation via Fully Convolutional Representation Learning,” presented at the Proceedings of the 5th ACM on International Conference on Multimedia Retrieval - ICMR '15, 2015.
- [55] *RSLLCR*. Available: <http://www.ihitworld.com/RSLCR.html>.